CHALMERS | UNIVERSITY OF GOTHENBURG

MASTER'S THESIS

Comparing the Streamline Diffusion Method and Bipartition Model for Electron Transport

JIPING XIN

Department of Mathematical Sciences
Division of Mathematics
CHALMERS UNIVERSITY OF TECHNOLOGY
UNIVERSITY OF GOTHENBURG
Gothenburg, Sweden 2008

Thesis for the Degree of Master of Science

Comparing the Streamline Diffusion Method and Bipartition Model for Electron Transport

Jiping Xin

Department of Mathematical Sciences
Division of Mathematics
Chalmers University of Technology and University of Gothenburg
SE – 412 96 Gothenburg, Sweden
Gothenburg, May 2008

COMPARING THE STREAMLINE DIFFUSION METHOD AND BIPARTITION MODEL FOR ELECTRON TRANSPORT

JIPING XIN

Abstract. In this thesis we derive the Fokker-Planck equation, by asymptotic approximation, from 1-50 MeV electron transport equation with the scattering power, stopping power and energy loss straggling and prove that this approximation is accurate. We simplify the equation using broad beam model and solve the resulting equation by the streamline diffusion finite element method (Sd-method). We compare our results for the energy and angular distributions with those from bipartition model and Monte Carlo simulations.

1. Introduction

This thesis is a part of the work on a series of two papers [1, 2] about the application of finite element methods (FEM) in radiation therapy. Radiation treatment planning is based on the study of transport equation, where both neutral (photon: x-ray) and charged particles (electron, ion, proton) are used. The mathematical approach and numerical analysis of transport equations used in radiation therapy is limited to Fourier type techniques or, e.g. finite difference and Monte Carlo methods. FEM is based on variational formulation and can be used to solve more general PDEs. Moreover it is more easily adapted to the complex geometries of the underlying domains. So we want to introduce FEM to this field. We start with the electron transport equation, for 1-50 MeV, given by [7]:

$$
\begin{aligned}
\mathbf{u}\cdot\triangledown f(\mathbf{r},\mathbf{u},E) =& \frac{N_A D}{A}\int_{4\pi}[f(\mathbf{r},\mathbf{u}',E)-f(\mathbf{r},\mathbf{u},E)]\sigma_N(E,\mathbf{u}\cdot\mathbf{u}')d\mathbf{u}' \\
&+\frac{N_A D}{A}\int_E^{E_0} f(\mathbf{r},\mathbf{u},E')\sigma_r(E',E'-E)dE' - \frac{N_A D}{A}\int_0^E f(\mathbf{r},\mathbf{u},E)\sigma_r(E,E-E')dE' \\
&+\frac{N_A D}{A}Z\int_E^{E_0}\int_{4\pi} f(\mathbf{r},\mathbf{u}',E')\sigma_M(E',E'-E)\delta[\mathbf{u}\cdot\mathbf{u}'-\varphi(E',E'-E)]d\mathbf{u}'dE' \\
&-\frac{N_A D}{A}Z\int_{E/2}^{E}\int_{4\pi} f(\mathbf{r},\mathbf{u},E)\sigma_M(E,E-E')\delta[\mathbf{u}\cdot\mathbf{u}'-\varphi(E,E-E')]d\mathbf{u}'dE' \\
&+S(\mathbf{r},\mathbf{u},E).
\end{aligned}
\tag{1}
$$

Date: May 22, 2008.

Key words and phrases. electron, linear transport equation, Fokker-Planck equation, broad beam model, bipartition model, streamline diffusion method, energy distribution and angle distribution.

Jiping Xin, Department of Mathematics, Chalmers University of Technology, SE–412 96 Göteborg, Sweden, *Email*: jiping@student.chalmers.se

.

To adopt to the current energy range, we need to consider certain key properties such as the influence of the elastic scattering, bremsstrahlung, and inelastic scattering and the continuous-slowing-down approximation (CSDA). In (1) N_A is Avogadro's number ($6.022045 \times 10^{23} mol^{-1}$), Z and A are the atomic number and atomic weight for the atom respectively, and D is the density for the medium.

To continue we need to introduce the cross sections for the elastic scattering, inelastic scattering and bremsstrahlung. (i) *The screened Rutherford cross section* is the cross section differential in the cosine ξ of the polar scattering angle of electrons or positrons incident on atoms of atomic number Z. A more accurate formula is obtained by considering the screening effect on the electric field of the nuclei resulting from the electron cloud outside nuclei, the inelastic scattering, and the relativistic effect. Because water is a typical medium in our calculation, the relevant elastic scattering cross section is the McKinley-Feshbach formula given in [14], as

$$\sigma_N(E,\xi) = \frac{r_0^2 Z(Z+1)(m_0c^2)^2(E+m_0c^2)^2}{E^2(E+2m_0c^2)^2}\left[\frac{1}{(1-\xi+2\eta)^2} + \frac{\pi\beta}{\sqrt{2}}\frac{Z}{137}\frac{1}{(1-\xi)^{3/2}} - \frac{1}{2}\left(\beta^2 + \frac{\pi\beta Z}{137}\right)\frac{1}{1-\xi}\right], \tag{2}$$

$$\eta = \frac{1}{4}\left[\frac{Z^{1/3}}{121.25}\right]^2\left[1.13 + 3.76\left(\frac{Z}{137}\right)^2\frac{(E+m_0c^2)^2}{E(E+2m_0c^2)}\right]\frac{(m_0c^2)^2}{E(E+2m_0c^2)}, \tag{3}$$

$$\beta = \frac{\sqrt{E(E+2m_0c^2)}}{E+m_0c^2}, \tag{4}$$

where η is the Moliere screen factor, see [15], r_0 is the classical electron radius ($2.817938 \times 10^{-15}\ m$), m_0c^2 is the relative rest mass ($0.511\ MeV$), and β is the particle velocity in units of the speed of light.

(ii) *The bremsstrahlung cross section* for an electron with a total energy E incident on an atom with atomic number Z is given, see [16], by

$$\sigma_r(E,T) = \frac{4r_0^2 Z^2}{137T}\left[\left(1 + \frac{(E-T)^2}{E^2} - \frac{2}{3}\frac{E-T}{E}\right)\left(\frac{\phi_1(\gamma)}{4} - \frac{1}{3}\ln Z\right) + \frac{E-T}{6E}\Delta(\gamma)\right], \tag{5}$$

$$\gamma = 100\frac{m_0c^2T}{E(E-T)Z^{1/3}}, \tag{6}$$

$$\phi_1(\gamma) = a_1 e^{-a_2\gamma} + b_1 e^{-b_2\gamma}, \tag{7}$$

$$\Delta(\gamma) = c_1 e^{-c_2\gamma} + d_1 e^{-d_2\gamma}, \tag{8}$$

where $E' = E - T$ is the electron energy after the emission of the photon with the energy T. The coefficients a_1=6.892, a_2=0.4813, b_1=13.817, b_2=0.03289, c_1=0.2592, c_2=2.869, d_1=13.817, and d_2=0.03289 are given parameters.

(iii) *The Moller cross section*, which is the cross section for electron-electron scattering differential in the kinetic energy T of the scattered electron which is initially at rest, is given in ICRU report, by the formula

$$\sigma_M(E,T) = \frac{r_0^2 m_0c^2(E+m_0c^2)^2}{E(E+2m_0c^2)}\frac{1}{T^2}\left[1 + \frac{T^2}{(E-T)^2} + \frac{E^2}{(E+m_0c^2)^2}\left(\frac{T}{E}\right)^2 - \frac{(2E+m_0c^2)m_0c^2}{(E+m_0c^2)^2}\frac{T}{E-T}\right], \tag{9}$$

where E is the incident kinetic energy.

The polar scattering angles, θ for the higher energy electron and θ' for the lower energy electron in Moller events, are uniquely determined by the kinematics. They are given by

$$\cos\theta = \left(\frac{E-T}{E}\frac{E+2m}{E-T+2m}\right)^{1/2}, \tag{10}$$

$$\cos\theta' = \left(\frac{T}{E}\frac{E+2m}{T+2m}\right)^{1/2}. \tag{11}$$

An outline of this thesis is as follows: In Section 2.1, we derive the Fokker-Planck equation for (1) with the scattering power, stopping power and energy loss straggling and check the accuracy. In Section 2.2, we define the broad beam model (BBM) and 2D pencil beam model (2PBM). In Section 2.3, we give a brief introduction of the bipartition model and compare it with the Fokker-Planck equation. In Section 3, we define the boundary conditions for BBM and use Sd-method to solve it. At the end of Section 3 we compare our results for the energy and angular distributions with those obtained by the bipartition model and Monte Carlo.

2. Fokker-Planck equation and bipartition model

2.1. **Fokker-Planck equation.** The classical contributions about the Fokker-Planck approximation are summarized by Chandrasekhar in [28] and Rosenbluth in [32]. [29, 31, 30] are studying the case of the linear particle transport. These works give a heuristic derivation of the Fokker-Planck operator. In [33] Pomraning gave a formalized derivation of the Fokker-Planck operator as an asymptotic limit of the integral scattering operator where a peaked scattering kernel is a necessary but not sufficient condition in the asymptotic treatment. Pomraning also gave an example by the Henyey-Greenstein kernel which is similar to the screened Rutherford cross section without corrections. He proved that the Henyey-Greenstein kernel, being "weakly forward-peaked", does not possess the Fokker-Planck operator as an asymptotic limit. In this section we give a derivation of the Fokker-Planck equation for 1-50 MeV electron transport equation (1) by Laplace method.

2.1.1. *Elastic scattering.* In this section we deal with the elastic scattering terms in (1):

$$\frac{N_A D}{A}\int_{4\pi}[f(\mathbf{r},\mathbf{u}',E)-f(\mathbf{r},\mathbf{u},E)]\sigma_N(E,\mathbf{u}\cdot\mathbf{u}')d\mathbf{u}'. \tag{12}$$

We expand $f(\mathbf{r},\mathbf{u}',E)$ in surface harmonics and $\sigma_N(E,\mathbf{u}\cdot\mathbf{u}')$ in Legendre polynomials about $\mathbf{u}\cdot\mathbf{u}'$ as [33],

$$f(\mathbf{r},\mathbf{u}',E) = \sum_{n=0}^{\infty}\sum_{m=-n}^{n}\left(\frac{2n+1}{4\pi}\right)a_{nm}f_{nm}(\mathbf{r},E)Y_{nm}(\mathbf{u}'), \tag{13}$$

$$\sigma_N(E,\mathbf{u}\cdot\mathbf{u}') = \sum_{k=0}^{\infty}\left(\frac{2k+1}{4\pi}\right)\sigma_{Nk}(E)P_k(\mathbf{u}\cdot\mathbf{u}'). \tag{14}$$

We shall use the following properties of surface harmonics and Legendre polynomials,

$$\int_{4\pi}Y_{nm}(\mathbf{u})Y^*_{kl}(\mathbf{u})d\mathbf{u} = \left(\frac{4\pi}{2n+1}\right)\left(\frac{1}{a_{nm}}\right)\delta_{nk}\delta_{ml}, \tag{15}$$

$$\left[\frac{\partial}{\partial\mu}(1-\mu^2)\frac{\partial}{\partial\mu}+\left(\frac{1}{1-\mu^2}\right)\frac{\partial^2}{\partial\phi^2}+n(n+1)\right]Y_{nm}(\mathbf{u})=0, \tag{16}$$

$$P_k(\mathbf{u}\cdot\mathbf{u}')=\sum_{l=-k}^{k}a_{kl}Y_{kl}(\mathbf{u})Y_{kl}^*(\mathbf{u}'). \tag{17}$$

Using (13), (14) with (15), (17) in (12) gives

$$\int_{4\pi}f(\mathbf{r},\mathbf{u}',E)\sigma_N(E,\mathbf{u}\cdot\mathbf{u}')d\mathbf{u}'=\sum_{n=0}^{\infty}\sum_{m=-n}^{n}\left(\frac{2n+1}{2}\right)a_{nm}f_{nm}(\mathbf{r},E)Y_{nm}(\mathbf{u})\int_{-1}^{1}P_n(\xi)\sigma_N(E,\xi)d\xi. \tag{18}$$

To simplify (12) we consider

$$I=\int_{-1}^{1}P_n(\xi)\sigma_N(E,\xi)d\xi. \tag{19}$$

Choose $\epsilon\in(\xi_n,1)$. Here ξ_n is the largest positive root of the Legendre polynomial $P_n(\xi)$. We split I into two parts and compare them in the following way,

$$I=\int_{-1}^{\epsilon}P_n(\xi)\sigma_N(E,\xi)d\xi+\int_{\epsilon}^{1}P_n(\xi)\sigma_N(E,\xi)d\xi:=I_1+I_2, \tag{20}$$

$$\frac{|I_1|}{I_2}\le\lim_{a\to0+}\frac{\int_{-1}^{\epsilon}\sigma_N(E,\xi)d\xi}{P_n(\epsilon)\int_{\epsilon}^{1-a}\sigma_N(E,\xi)d\xi}=0. \tag{21}$$

Then we have $I\approx I_2$.

Choosing ϵ sufficiently close to 1, $P_n(\epsilon)$ is well approximated by it's first order Taylor expansion,

$$I_2\approx\int_{\epsilon}^{1}[P_n(1)+P_n^{(1)}(1)(\xi-1)]\sigma_N(E,\xi)d\xi:=I_2'. \tag{22}$$

Now we define I_1' and compare it with I_2',

$$I_1':=\int_{-1}^{\epsilon}[P_n(1)+P_n^{(1)}(1)(\xi-1)]\sigma_N(E,\xi)d\xi, \tag{23}$$

$$\frac{I_1'}{I_2'}=\lim_{a\to0+}\frac{\int_{-1}^{\epsilon}[P_n(1)+P_n^{(1)}(1)(\xi-1)]\sigma_N(E,\xi)d\xi}{\int_{\epsilon}^{1-a}[P_n(1)+P_n^{(1)}(1)(\xi-1)]\sigma_N(E,\xi)d\xi}=0. \tag{24}$$

Then we have

$$I\approx I_2\approx I_2'\approx I_2'+I_1'=\int_{-1}^{1}[P_n(1)+P_n^{(1)}(1)(\xi-1)]\sigma_N(E,\xi)d\xi. \tag{25}$$

We use (25), (16) in (18) and obtain

$$\begin{aligned}
&\frac{N_A D}{A}\sum_{n=0}^{\infty}\sum_{m=-n}^{n}\left(\frac{2n+1}{2}\right)a_{nm}f_{nm}(\mathbf{r},E)Y_{nm}(\mathbf{u})\int_{-1}^{1}[P_n(1)+P_n^{(1)}(1)(\xi-1)]\sigma_N(E,\xi)d\xi \\
&\qquad\qquad -\frac{N_A D}{A}f(\mathbf{r},\mathbf{u},E)\int_{4\pi}\sigma_N(E,\mathbf{u}\cdot\mathbf{u}')d\mathbf{u}' \\
&=\frac{N_A D}{A}f(\mathbf{r},\mathbf{u},E)\int_{4\pi}\sigma_N(E,\mathbf{u}\cdot\mathbf{u}')d\mathbf{u}'+T_1(E)\left[\frac{\partial}{\partial\mu}(1-\mu^2)\frac{\partial}{\partial\mu}+\frac{1}{1-\mu^2}\frac{\partial^2}{\partial\phi^2}\right]f(\mathbf{r},\mathbf{u},E) \\
&\qquad\qquad -\frac{N_A D}{A}f(\mathbf{r},\mathbf{u},E)\int_{4\pi}\sigma_N(E,\mathbf{u}\cdot\mathbf{u}')d\mathbf{u}' \\
&=T_1(E)\left[\frac{\partial}{\partial\mu}(1-\mu^2)\frac{\partial}{\partial\mu}+\frac{1}{1-\mu^2}\frac{\partial^2}{\partial\phi^2}\right]f(\mathbf{r},\mathbf{u},E),
\end{aligned}\tag{26}$$

$$T_1(E)=\frac{N_A D}{A}\pi\int_{-1}^{1}(1-\xi)\sigma_N(E,\xi)d\xi. \tag{27}$$

$T_1(E)$ is the scattering power which expresses the increase in mean square angle of scattering per unit mass thickness. Replacing the expression of $\sigma_N(E,\xi)$ from (2), we can easily compute $T_1(E)$, see Fig. 1,

$$T_1(E)=\frac{N_A D}{A}\pi\frac{r_0^2 Z(Z+1)(m_0c^2)^2(E+m_0c^2)^2}{E^2(E+2m_0c^2)^2}\left(-\frac{1}{1+\eta}-\ln\frac{\eta}{1+\eta}+\frac{\pi\beta Z}{137}-\beta^2\right). \tag{28}$$

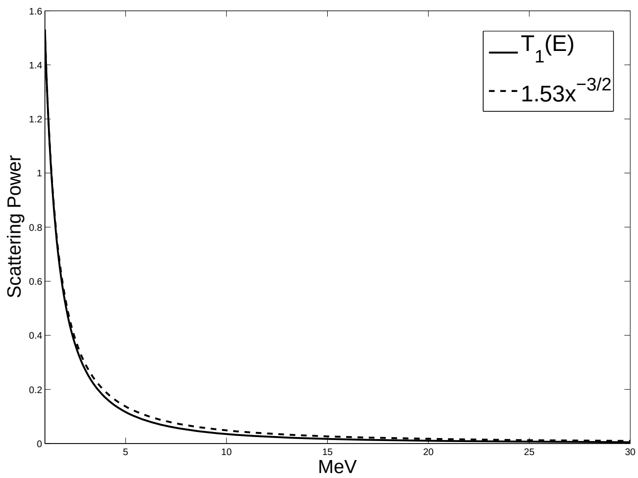

FIGURE 1. Scattering power for elastic scattering

On the other hand for the screened Rutherford cross section without corrections, the formula (29) below, we could follow the same steps and find that the Fokker-Planck operator is not an accurate asymptotic approximation of the integral operator. The reason is that I_2 converges to 0 as ϵ tends to 1:

$$\sigma_N(\xi,T)=\frac{r_0^2 Z^2}{\beta^2\tau(\tau+2)}\frac{1}{(1-\xi+2\eta)^2} \tag{29}$$

$$I_2 = \int_\epsilon^1 P_n(\xi)\sigma_N(E,\xi)d\xi \le \int_\epsilon^1 \sigma_N(E,\xi)d\xi = \frac{r_0^2 Z^2}{\beta^2\tau(\tau+2)}\left(\frac{1}{2\eta} - \frac{1}{1-\epsilon+2\eta}\right) \to 0 \quad as \ \ \epsilon \to 1. \tag{30}$$

2.1.2. *Bremsstrahlung.* In this section we deal with the bremsstrahlung terms in (1):

$$\frac{N_A D}{A}\int_E^{E_0} f(\mathbf{r},\mathbf{u},E')\sigma_r(E',E'-E)dE' - \frac{N_A D}{A}\int_0^E f(\mathbf{r},\mathbf{u},E)\sigma_r(E,E-E')dE' := \tilde{I} + \tilde{I}I. \tag{31}$$

To continue we define the function $A(E',T)$ by

$$\begin{aligned} A(E',T) &= max\left\{\frac{4r_0^2Z^2}{137}\left[\left(1+\frac{(E'-T)^2}{E'^2} - \frac{2}{3}\frac{E'-T}{E'}\right)\left(\frac{\phi_1(\gamma)}{4} - \frac{1}{3}\ln Z\right) + \frac{E'-T}{6E'}\Delta(\gamma)\right], 0\right\}, \qquad Z = 8,\\ A(E',T) &= \frac{4r_0^2Z^2}{137}\left[\left(1+\frac{(E'-T)^2}{E'^2} - \frac{2}{3}\frac{E'-T}{E'}\right)\left(\frac{\phi_1(\gamma)}{4} - \frac{1}{3}\ln Z\right) + \frac{E'-T}{6E'}\Delta(\gamma)\right], \qquad Z = 1, \end{aligned} \tag{32}$$

where $T = E' - E$ and $Z = 1$ and $Z = 8$ are the atom numbers of H and O, respectively (the atoms in the molecule of water). Then we have

$$\sigma_r(E',T) = \frac{A(E',T)}{T}. \tag{33}$$

From (32) and the definition of $\phi_1(\gamma)$ and $\Delta(\gamma)$ in (7) and (8), we conclude that $A(E',T)$ is a nonnegative continuous function in $[E, E_0]$. To simplify (31) we consider $\tilde{I}$ and choose $\epsilon \in (E, E_0)$ such that $A(E',T)$ is positive in $[E,\epsilon]$ and split $\tilde{I}$ into two parts,

$$\tilde{I} = \frac{N_A D}{A}\int_E^{\epsilon} f(\mathbf{r},\mathbf{u},E')\sigma_r(E',T)dE' + \frac{N_A D}{A}\int_\epsilon^{E_0} f(\mathbf{r},\mathbf{u},E')\sigma_r(E',T)dE' := \tilde{I}_1 + \tilde{I}_2. \tag{34}$$

Since $f(\mathbf{r},\mathbf{u},E')$ is the particle phase space density, we may assume that it is a continuous positive function on $[E, E_0]$. Then we have

$$\frac{\tilde{I}_2}{\tilde{I}_1} \le \frac{max_{E'\in[\epsilon,E_0]}(f(\mathbf{r},\mathbf{u},E')A(E',T))}{min_{E'\in[E,\epsilon]}(f(\mathbf{r},\mathbf{u},E')A(E',T))}\lim_{a\to 0+}\frac{\int_\epsilon^{E_0}\frac{1}{T}dE'}{\int_{E+a}^{\epsilon}\frac{1}{T}dE'} = 0. \tag{35}$$

Thus, compared to $\tilde{I}_1$, $\tilde{I}_2$ is negligible and we can write $\tilde{I} \approx \tilde{I}_1$.

Choosing ϵ sufficiently close to E, $f(\mathbf{r},\mathbf{u},E')A(E',T)$ is well approximated by it's second order Taylor expansion about $E' = E$,

$$\begin{aligned} \tilde{I}_1 \approx& \frac{N_A D}{A}\int_E^{\epsilon}\left\{f(\mathbf{r},\mathbf{u},E)A(E,T) + \left[\frac{\partial}{\partial E}f(\mathbf{r},\mathbf{u},E)A(E,T)\right]T + \frac{1}{2}\left[\frac{\partial^2}{\partial E^2}f(\mathbf{r},\mathbf{u},E)A(E,T)\right]T^2\right\}\frac{1}{T}dE' \\ :=& A_1 + A_2 + A_3 := \tilde{I}_1' \end{aligned} \tag{36}$$

It is easy to check that $A(E,T)$ is positive in $[E,\epsilon]$, and $A(E,T)$, $\frac{\partial A(E,T)}{\partial E}$ and $\frac{\partial^2 A(E,T)}{\partial E^2}$ are continuous functions on $[E, 2E]$. We define $\tilde{I}_2'$ by

$$\begin{aligned} \tilde{I}_2' =& \frac{N_A D}{A}\int_\epsilon^{2E}\left\{f(\mathbf{r},\mathbf{u},E)A(E,T) + \left[\frac{\partial}{\partial E}f(\mathbf{r},\mathbf{u},E)A(E,T)\right]T + \frac{1}{2}\left[\frac{\partial^2}{\partial E^2}f(\mathbf{r},\mathbf{u},E)A(E,T)\right]T^2\right\}\frac{1}{T}dE' \\ :=& A_1' + A_2' + A_3'. \end{aligned} \tag{37}$$

We assume that $f(\mathbf{r},\mathbf{u},E)\in C^2([E,2E])$. So for $T\to 0$, $A_1\to\infty$ and A_2, A_3, A_1', A_2', A_3' are bounded. Then we have

$$\frac{\tilde{I}_2'}{\tilde{I}_1'}=\frac{A_1'+A_2'+A_3'}{A_1+A_2+A_3}\to 0 \qquad as\;\; T\to 0. \tag{38}$$

Thus,

$$\begin{aligned}&\tilde{I}\approx\tilde{I}_1\approx\tilde{I}_1'\approx\tilde{I}_1'+\tilde{I}_2'\\ &=\frac{N_AD}{A}\int_E^{2E}\left\{f(\mathbf{r},\mathbf{u},E)A(E,T)+\left[\frac{\partial}{\partial E}f(\mathbf{r},\mathbf{u},E)A(E,T)\right]T+\frac{1}{2}\left[\frac{\partial^2}{\partial E^2}f(\mathbf{r},\mathbf{u},E)A(E,T)\right]T^2\right\}\frac{1}{T}dE'.\end{aligned} \tag{39}$$

Now using the change of variables as $E'-E=E-F'$ $(T'=E-F')$, we get

$$\begin{aligned}\tilde{I}&\approx\frac{N_AD}{A}\int_0^{E}\left\{f(\mathbf{r},\mathbf{u},E)A(E,T')+\left[\frac{\partial}{\partial E}f(\mathbf{r},\mathbf{u},E)A(E,T')\right]T'+\frac{1}{2}\left[\frac{\partial^2}{\partial E^2}f(\mathbf{r},\mathbf{u},E)A(E,T')\right]T'^2\right\}\frac{1}{T'}dF'\\ &=\frac{N_AD}{A}\int_0^{E}f(\mathbf{r},\mathbf{u},E)\sigma_r(E,T')dF'+\frac{\partial}{\partial E}f(\mathbf{r},\mathbf{u},E)S_1(E)+\frac{\partial^2}{\partial E^2}f(\mathbf{r},\mathbf{u},E)R_1(E),\end{aligned} \tag{40}$$

$$S_1(E)=\frac{N_AD}{A}\int_0^{E}\sigma_r(E,T')T'dF', \tag{41}$$

$$R_1(E)=\frac{N_AD}{2A}\int_0^{E}\sigma_r(E,T')T'^2dF'. \tag{42}$$

We return to the notation E' (instead of F') and insert (40) in (31) to obtain:

$$\begin{aligned}\tilde{I}+\tilde{I}I\approx&\frac{N_AD}{A}\int_0^{E}f(\mathbf{r},\mathbf{u},E)\sigma_r(E,T)dE'+\frac{\partial}{\partial E}f(\mathbf{r},\mathbf{u},E)S_1(E)+\frac{\partial^2}{\partial E^2}f(\mathbf{r},\mathbf{u},E)R_1(E)\\ &-\frac{N_AD}{A}\int_0^{E}f(\mathbf{r},\mathbf{u},E)\sigma_r(E,T)dE'=\frac{\partial}{\partial E}f(\mathbf{r},\mathbf{u},E)S_1(E)+\frac{\partial^2}{\partial E^2}f(\mathbf{r},\mathbf{u},E)R_1(E).\end{aligned} \tag{43}$$

Here $S_1(E)$ is the stopping power and $R_1(E)$ is the energy losss straggling. We calculate $S_1(E)$ and $R_1(E)$ and find out that we could use $0.022E$ as an approximation for $S_1(E)$.

In [7] Luo used the radiation stopping power given in [17] and the fitting formula for φ_{rad} given in [18] by Seltzer and Berger,

$$S_{rad}(E)=\frac{N_AD}{A}Z(Z+1)\frac{r_0^2}{137}(E+m_0c^2)\varphi_{rad}, \tag{44}$$

$$R_{rad}(E)=\frac{N_AD}{A}\int_0^{E}\sigma_r(E,T)T^2dT\approx(\alpha_1+\alpha_2E^{\alpha_3})ES_{rad}, \tag{45}$$

where, for water, $\alpha_1=0.3$, $\alpha_2=0.02226$ and $\alpha_3=0.35655$.

2.1.3. *Inelastic scattering.* In this section we deal with inelastic scattering terms in (1):

$$\begin{aligned}\sum:=&\frac{N_AD}{A}Z\int_E^{E_0}\int_{4\pi}f(\mathbf{r},\mathbf{u}',E')\sigma_M(E',E'-E)\delta[\mathbf{u}\cdot\mathbf{u}'-\varphi(E',E'-E)]d\mathbf{u}'dE'\\ &-\frac{N_AD}{A}Z\int_{E/2}^{E}\int_{4\pi}f(\mathbf{r},\mathbf{u},E)\sigma_M(E,E-E')\delta[\mathbf{u}\cdot\mathbf{u}'-\varphi(E,E-E')]d\mathbf{u}'dE'.\end{aligned} \tag{46}$$

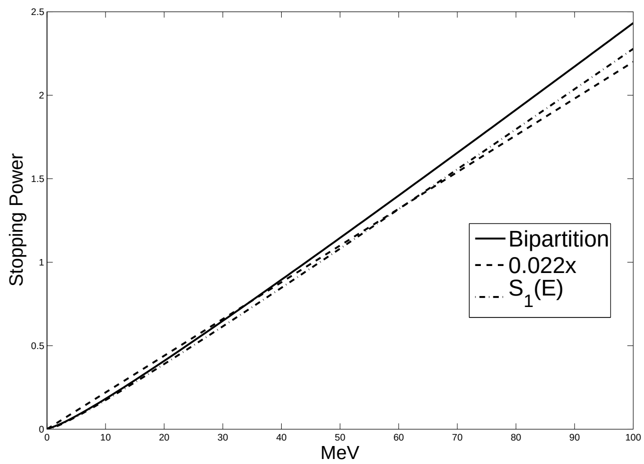

FIGURE 2. Stopping power for bremsstrahlung

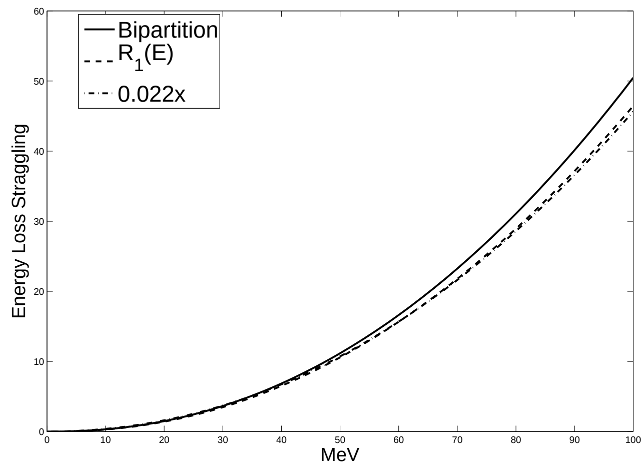

FIGURE 3. Energy loss straggling for bremsstrahlung

We extend $f(\mathbf{r}, \mathbf{u}', E')$ in spherical harmonics and $\sigma_M(E',T)\delta\left[\mathbf{u}\cdot\mathbf{u}' - \varphi(E',T)\right]$ in Legendre polynomials. To this end we let $T = E' - E$ and write

$$f(\mathbf{r}, \mathbf{u}', E') = \sum_{n=0}^{\infty}\sum_{m=-n}^{n}\left(\frac{2n+1}{4\pi}\right) a_{nm} f_{nm}(\mathbf{r}, E') Y_{nm}(\mathbf{u}'), \tag{47}$$

$$\sigma_M(E',T)\delta\left[\mathbf{u}\cdot\mathbf{u}' - \varphi(E',T)\right] = \sigma_M(E',T)\sum_{k=0}^{\infty}\left(\frac{2k+1}{2}\right) P_k(\mathbf{u}\cdot\mathbf{u}') P_k\left[\varphi(E',T)\right]. \tag{48}$$

Using (47) and (48) with (15) and (17) in (46), yields

$$\begin{aligned}&\frac{N_A d}{A} Z \int_E^{E_0} \int_{4\pi} f(\mathbf{r}, \mathbf{u}', E')\sigma_M(E', E'-E)\delta\left[\mathbf{u}\cdot\mathbf{u}' - \varphi(E', E'-E)\right] d\mathbf{u}' dE' \\ &= \frac{N_A D}{A} Z \sum_{n=0}^{\infty}\sum_{m=-n}^{n}\left(\frac{2n+1}{2}\right) a_{nm} Y_{nm}(\mathbf{u}) \int_E^{E_0}\int_{-1}^{1} f_{nm}(\mathbf{r}, E')P_n(\xi)\sigma_M(E', T)\delta\left[\xi - \varphi(E', T)\right] d\xi dE'.\end{aligned} \tag{49}$$

To simplify (46) we consider the integral

$$\hat{I} = \int_E^{E_0}\int_{-1}^{1} f_{nm}(\mathbf{r}, E')P_n(\xi)\sigma_M(E', T)\delta\left[\xi - \varphi(E', T)\right] d\xi dE', \tag{50}$$

and define

$$A(E', T) = \frac{r_0^2 m_0 c^2 (E' + m_0c^2)^2}{E'(E' + 2m_0c^2)}\left[1 + \frac{T^2}{(E'-T)^2} + \frac{E'^2}{(E'+m_0c^2)^2}\left(\frac{T}{E'}\right)^2 - \frac{(2E'+m_0c^2)m_0c^2}{(E'+m_0c^2)^2}\frac{T}{E'-T}\right]. \tag{51}$$

$A(E', T)$ is a positive continuous function in $[E, E_0]$ and we have

$$\sigma_M(E', T) = \frac{A(E', T)}{T^2}. \tag{52}$$

Since $\varphi(E', T)$ tends to 1 as E' tends to E, we define ϵ_1 and ϵ_2 such that $\xi_n < \epsilon_2 < \varphi(E', T)$ for $E' \in [E, \epsilon_1]$. ξ_n is the largest positive root of $P_n(\xi)$ in $(0, 1)$. We split $\hat{I}$ into the following three parts:

$$\begin{aligned}\hat{I} =& \int_E^{\epsilon_1}\int_{\epsilon_2}^{1} f_{nm}(\mathbf{r}, E')P_n(\xi)\frac{A(E', T)}{T^2}\delta\left[\xi - \varphi(E', T)\right] d\xi dE' \\ &+ \int_E^{\epsilon_1}\int_{-1}^{\epsilon_2} f_{nm}(\mathbf{r}, E')P_n(\xi)\frac{A(E', T)}{T^2}\delta\left[\xi - \varphi(E', T)\right] d\xi dE' \\ &+ \int_{\epsilon_1}^{E_0}\int_{-1}^{1} f_{nm}(\mathbf{r}, E')P_n(\xi)\frac{A(E', T)}{T^2}\delta\left[\xi - \varphi(E', T)\right] d\xi dE' := \hat{I}_1 + \hat{I}_2 + \hat{I}_3.\end{aligned} \tag{53}$$

Since $\xi_n < \epsilon_2 < \varphi(E', E)$ for $E' \in [E, \epsilon_1]$, $\hat{I}_2 = 0$. We compare $\hat{I}_1$ and $\hat{I}_3$,

$$\frac{\hat{I}_3}{\hat{I}_1} \le \frac{\max_{E' \in [E, E_0]}\left[f_{nm}(\mathbf{r}, E')A(E', T)\right]\int_{\epsilon_1}^{E_0}\frac{1}{T^2}dE'}{\min_{E' \in [E, E_0]}\left[f_{nm}(\mathbf{r}, E')A(E', T)\right]P_n(\epsilon_2)\int_E^{\epsilon_1}\frac{1}{T^2}dE'} = 0, \tag{54}$$

and conclude that $\hat{I} \approx \hat{I}_1$.

Choosing ϵ_1 and ϵ_2 sufficiently close to E and 1 respectively, $f_{nm}(\mathbf{r}, E')A(E', T)$ is well approximated by it's second order Taylor expansion about $E' = E$ and $P_n(\xi)$ is well approximated by it's first order Taylor expansion about $\xi = 1$. Thus

$$
\begin{aligned}
\hat{I}_1 \approx & \int_E^{\epsilon_1} \int_{\epsilon_2}^1 \left\{ f_{nm}(\mathbf{r}, E)A(E,T) + \left[\frac{\partial}{\partial E} f_{nm}(\mathbf{r}, E)A(E,T)\right] T + \left[\frac{1}{2}\frac{\partial^2}{\partial E^2} f_{nm}(\mathbf{r}, E)A(E,T)\right] T^2 \right\} \cdot \\
& \left[1 + P_n^{(1)}(1)(\xi - 1)\right] \frac{1}{T^2} \delta\left[\xi - \varphi(E',T)\right] d\xi dE' \\
= & \int_E^{\epsilon_1} f_{nm}(\mathbf{r}, E)A(E,T)\frac{1}{T^2} dE' + \int_E^{\epsilon_1} \left[\frac{\partial}{\partial E} f_{nm}(\mathbf{r}, E)A(E,T)\right] \frac{1}{T} dE' \\
& + \int_E^{\epsilon_1} \frac{1}{2}\frac{\partial^2}{\partial E^2} f_{nm}(\mathbf{r}, E)A(E,T) dE' + \int_E^{\epsilon_1} f_{nm}(\mathbf{r}, E)A(E,T)P_n^{(1)}(1)\frac{[\varphi(E',T) - 1]}{T^2} dE' \\
& + \int_E^{\epsilon_1} \left[\frac{\partial}{\partial E} f_{nm}(\mathbf{r}, E)A(E,T)\right] P_n^{(1)}(1) \frac{[\varphi(E',T) - 1]}{T} dE' \\
& + \int_E^{\epsilon_1} \left[\frac{1}{2}\frac{\partial^2}{\partial E^2} f_{nm}(\mathbf{r}, E)A(E,T)\right] P_n^{(1)}(1) \left[\varphi(E',T) - 1\right] dE' := J_1 + J_2 + J_3 + J_4 + J_5 + J_6.
\end{aligned} \tag{55}
$$

One can easily check that $A(E,T)$, $\frac{\partial A(E,T)}{\partial E}$, $\frac{\partial^2 A(E,T)}{\partial E^2}$ and $\varphi(E',T)$ are continuous functions in $[E, \frac{3}{2}E]$ and $\lim_{E' \to E} \frac{[\varphi(E',T)-1]}{T^2} = \infty$, $\lim_{E' \to E} \frac{[\varphi(E',T)-1]}{T} < \infty$. In this way we have $J_4 \to \infty$ and J_5, J_6 are bounded. Since ϵ_1 sufficiently closes to E, $\varphi(E',T)$ is well approximated by $\varphi(E,T)$. Then, obviously

$$
\hat{I}_1 \approx J_1 + J_2 + J_3 + J_4 := \hat{I}_1'. \tag{56}
$$

Now we define

$$
\begin{aligned}
\hat{I}_2' = & \int_E^{\epsilon_1} \int_{-1}^{\epsilon_2} f_{nm}(\mathbf{r}, E)A(E,T)\frac{1}{T^2}\delta[\xi - \varphi(E,T)] d\xi dE' \\
& + \int_E^{\epsilon_1} \int_{-1}^{\epsilon_2} \left[\frac{\partial}{\partial E} f_{nm}(\mathbf{r}, E)A(E,T)]\right] T \frac{1}{T^2}\delta[\xi - \varphi(E,T)] d\xi dE' \\
& + \int_E^{\epsilon_1} \int_{-1}^{\epsilon_2} \left[\frac{1}{2}\frac{\partial^2}{\partial E^2} f_{nm}(\mathbf{r}, E)A(E,T)]\right] T^2 \frac{1}{T^2}\delta[\xi - \varphi(E,T)] d\xi dE' \\
& + \int_E^{\epsilon_1} \int_{-1}^{\epsilon_2} f_{nm}(\mathbf{r}, E)A(E,T)P_n^{(1)}(1)(\xi - 1)\frac{1}{T^2}\delta[\xi - \varphi(E,T)] d\xi dE',
\end{aligned} \tag{57}
$$

$$
\begin{aligned}
\hat{I}_3' = & \int_{\epsilon_1}^{\frac{3}{2}E} \int_{-1}^{1} f_{nm}(\mathbf{r}, E)A(E,T)\frac{1}{T^2}\delta[\xi - \varphi(E,T)] d\xi dE' \\
& + \int_{\epsilon_1}^{\frac{3}{2}E} \int_{-1}^{1} \left[\frac{\partial}{\partial E} f_{nm}(\mathbf{r}, E)A(E,T)]\right] T \frac{1}{T^2}\delta[\xi - \varphi(E,T)] d\xi dE' \\
& + \int_{\epsilon_1}^{\frac{3}{2}E} \int_{-1}^{1} \left[\frac{1}{2}\frac{\partial^2}{\partial E^2} f_{nm}(\mathbf{r}, E)A(E,T)]\right] T^2 \frac{1}{T^2}\delta[\xi - \varphi(E,T)] d\xi dE' \\
& + \int_{\epsilon_1}^{\frac{3}{2}E} \int_{-1}^{1} f_{nm}(\mathbf{r}, E)A(E,T)P_n^{(1)}(1)(\xi - 1)\frac{1}{T^2}\delta[\xi - \varphi(E,T)] d\xi dE'.
\end{aligned} \tag{58}
$$

It is easy to check that $\hat{I}'_2 = 0$ and $\hat{I}'_3$ is bounded. Then we have

$$
\begin{aligned}
&\hat{I} \approx \hat{I}_1 \approx \hat{I}'_1 \approx \hat{I}'_1 + \hat{I}'_2 + \hat{I}'_3 = \hat{I}' \\
&= \int_E^{\frac{3}{2}E} \int_{-1}^{1} f_{nm}(\mathbf{r}, E) A(E,T) \frac{1}{T^2} \delta[\xi - \varphi(E,T)] d\xi dE' \\
&+ \int_E^{\frac{3}{2}E} \int_{-1}^{1} \left[\frac{\partial}{\partial E} f_{nm}(\mathbf{r}, E) A(E,T) \right] T \frac{1}{T^2} \delta[\xi - \varphi(E,T)] d\xi dE' \\
&+ \int_E^{\frac{3}{2}E} \int_{-1}^{1} \left[\frac{1}{2} \frac{\partial^2}{\partial E^2} f_{nm}(\mathbf{r}, E) A(E,T) \right] T^2 \frac{1}{T^2} \delta[\xi - \varphi(E,T)] d\xi dE' \\
&+ \int_E^{\frac{3}{2}E} \int_{-1}^{1} f_{nm}(\mathbf{r}, E) A(E,T) P_n^{(1)}(1)(\xi - 1) \frac{1}{T^2} \delta[\xi - \varphi(E,T)] d\xi dE'.
\end{aligned} \tag{59}
$$

We change the integration variables from E' to F' according to $E' - E = E - F'$,

$$
\begin{aligned}
\hat{I}' = &\int_{\frac{1}{2}E}^{E} \int_{-1}^{1} f_{nm}(\mathbf{r}, E) \frac{A(E,T')}{T'^2} \delta[\xi - \varphi(E,T')] d\xi dF' \\
&+ \int_{\frac{1}{2}E}^{E} \int_{-1}^{1} \left[\frac{\partial}{\partial E} f_{nm}(\mathbf{r}, E) A(E,T') \right] T' \frac{1}{T'^2} \delta[\xi - \varphi(E,T')] d\xi dF' \\
&+ \int_{\frac{1}{2}E}^{E} \int_{-1}^{1} \left[\frac{1}{2} \frac{\partial^2}{\partial E^2} f_{nm}(\mathbf{r}, E) A(E,T') \right] T'^2 \frac{1}{T'^2} \delta[\xi - \varphi(E,T')] d\xi dF' \\
&+ \int_{\frac{1}{2}E}^{E} \int_{-1}^{1} f_{nm}(\mathbf{r}, E) A(E,T') P_n^{(1)}(1)(\xi - 1) \frac{1}{T'^2} \delta[\xi - \varphi(E,T')] d\xi dF',
\end{aligned} \tag{60}
$$

where $T' = E - F'$.

Below we shall keep using the notation E' and T instead of F' and T'. Then by using (60) in (46) denoted by $\sum$, we have:

$$
\sum \approx T_2(E) \left[\frac{\partial}{\partial \mu}(1-\mu^2)\frac{\partial}{\partial \mu} + \frac{1}{1-\mu^2}\frac{\partial^2}{\partial \phi^2} \right] f(\mathbf{r}, \mathbf{u}, E) + \frac{\partial}{\partial E}\left[S_2(E) f(\mathbf{r}, \mathbf{u}, E)\right] + \frac{\partial^2}{\partial E^2}\left[R_2(E) f(\mathbf{r}, \mathbf{u}, E)\right], \tag{61}
$$

$$
S_2(E) = 2\pi \int_{\frac{1}{2}E}^{E} \sigma_M(E,T) T dE', \tag{62}
$$

$$
R_2(E) = \pi \int_{\frac{1}{2}E}^{E} \sigma_M(E,T) T^2 dE', \tag{63}
$$

$$
T_2(E) = \pi \int_{\frac{1}{2}E}^{E} \int_{-1}^{1} \sigma_M(E,T) \delta[\xi - \varphi(E,T)](1-\xi) d\xi dE'. \tag{64}
$$

We calculate the stopping power and energy loss straggling for the inelastic scattering by using the formula (9). In the calculation we change the integral range $[E, \frac{1}{2}E]$ to $[E-a, \frac{1}{2}E]$. The reason is that the energy change of primary electrons must be larger than the binding energy in the inelastic scattering. Since the binding energy is very small, the asymptotic approximation is still accurate.

$$
\begin{aligned}
S_2(E) = &\frac{N_A D}{A} Z \frac{4\pi r_0^2 m_0 c^2 (E + m_0c^2)^2}{E(E + 2m_0c^2)} \cdot \\
&\left[-\ln(a) + \frac{E - 2a}{E - a} + \ln \frac{E^2}{4(E-a)} + \frac{1}{(E+m_0c^2)^2}\left(\frac{E^2}{8} - \frac{a^2}{2}\right) + \frac{(2E + m_0c^2)m_0c^2}{(E+m_0c^2)^2} \ln \frac{E}{2(E-a)} \right],
\end{aligned} \tag{65}
$$

$$R_2(E) \approx \frac{N_A D}{A} Z \frac{2\pi r_0^2 m_0 c^2 (E + m_0 c^2)^2}{E(E + 2m_0 c^2)} E \left[2 - 2\ln 2 + \frac{E^2}{24(E + m_0 c^2)^2} - \frac{(2E + m_0 c^2) m_0 c^2}{(E + m_0 c^2)^2} (\ln 2 - 0.5) \right]. \tag{66}$$

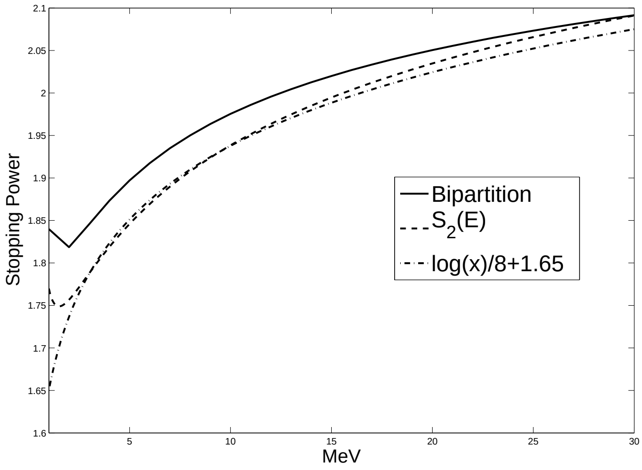

FIGURE 4. Stopping power for inelastic scattering

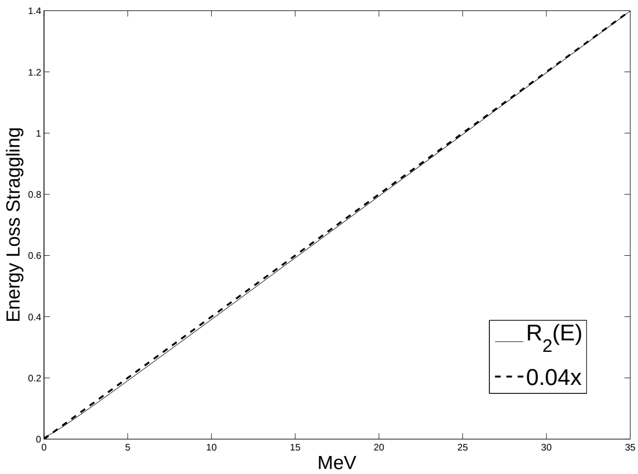

FIGURE 5. Energy loss straggling for inelastic scattering

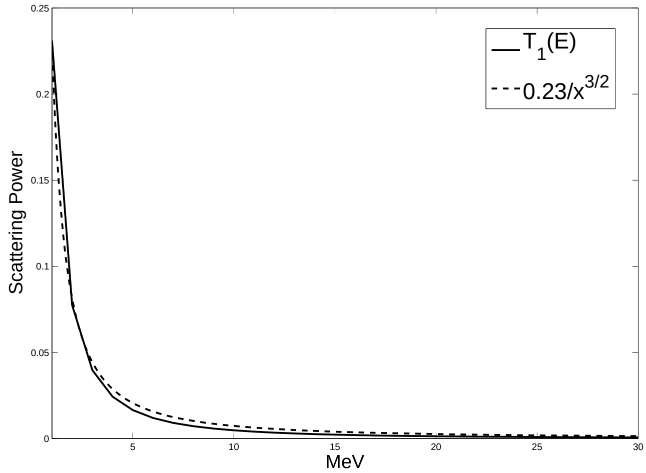

FIGURE 6. Scattering power for inelastic scattering

2.1.4. *Fokker-Planck equation.* Using the above results we have the following Fokker-Planck equation

$$\begin{aligned}\mathbf{u}\cdot\nabla f(\mathbf{r},\mathbf{u},E) =& T(E)\left[\frac{\partial}{\partial\mu}(1-\mu^2)\frac{\partial}{\partial\mu}+\left(\frac{1}{1-\mu^2}\right)\frac{\partial^2}{\partial\phi^2}\right]f(\mathbf{r},\mathbf{u},E)\\ &+\frac{\partial}{\partial E}[S(E)f(\mathbf{r},\mathbf{u},E)]+\frac{\partial^2}{\partial E^2}[R(E)f(\mathbf{r},\mathbf{u},E)],\end{aligned}\tag{67}$$

where $T(E)=T_1(E)+T_2(E)$, $S(E)=S_1(E)+S_2(E)$ and $R(E)=R_1(E)+R_2(E)$.

A general form of the Fokker-Planck equation for anisotropic media is derived in [23]. We should talk a littler about the Fermi equation which can be derived from (67) or the transport equation as in [35] and [37]. The main virtue of the application of the Fermi approximation in the dose calculation is that, by artificially extending the range of θ_x and θ_y to the entire real line, by Fourier transform with respect to y, z, θ_x and θ_y, we can obtain the exact solution. In this thesis, we want to show that FEM could solve more general equations. We concentrate on the Fokker Planck equation given by (67). The corresponding Fermi equation reads as the follows,

$$\frac{\partial f}{\partial z}+\theta_x\frac{\partial f}{\partial x}+\theta_y\frac{\partial f}{\partial y}=\frac{\partial S(E)f}{\partial E}+\frac{\partial^2 R(E)f}{\partial E^2}+T(E)\left(\frac{\partial^2 f}{\partial\theta_x^2}+\frac{\partial^2 f}{\partial\theta_y^2}\right).\tag{68}$$

2.2. **Broad beam model and 2D pencil beam model.** The Fokker-Planck equation (67) in Section 2.1.4 has six variables and it is not easy to solve it without some simplifications. The most comman way to simplify it is through considering either a broad beam model (BBM) or a 2D pencil beam model (2PBM). Below we give a brief introduction to these two models. Our work is devoted to the study of the broad beam model. To start we define the coordinate system for the position and direction variables in Figure 7 characterizing a classical point particle. We shall consistently use the notations in Figure 7.

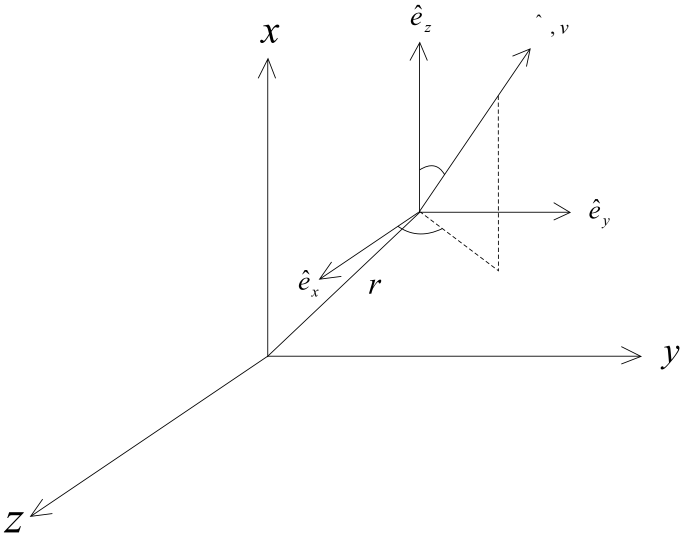

FIGURE 7. Coordinate system

2.2.1. *Broad Beam Model.* The construction of the bipartition model is based on BBM. We could consider it as a monoenergetic and monodirectional plane source embedded in an infinite homogeneous medium as in Fig. 8. We should emphasize that the emission direction of the source is paralled to x-axis. So by the symmetry $f(\mathbf{r}, \mathbf{u}, E)$ is independent of y, z and ϕ, and we may simplify the equation (67) to obtain the broad beam equation:

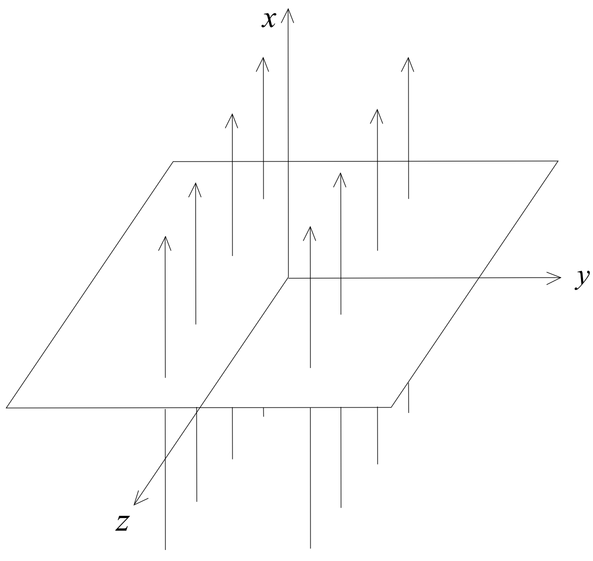

FIGURE 8. Broad beam

$$\mu \frac{\partial f(x,\mu,E)}{\partial x} = T(E)\frac{\partial}{\partial \mu}\left[(1-\mu^2)\frac{\partial}{\partial \mu} f(x,\mu,E)\right] + \frac{\partial}{\partial E}[S(E)f(x,\mu,E)] + \frac{\partial^2}{\partial E^2}[R(E)f(x,\mu,E)]. \tag{69}$$

Note that in this equation we have single space variable x and reduced the problem from being expressed in 6 dimensional to 3 dimensional.

2.2.2. *2D Pencil Beam Model.* The 2D pencil beam model has been used in Fermi-Eyges theory in [39, 40]. We may view it as a projection of 3D pencil beam model on yz-plane as Fig. 9. Note that the emission direction of the source is now paralled to the y-axis. Because if we use the same emission direction as Figure 8, then only μ will not be sufficient to characterize the particle phase density and we should still keep ϕ. But if we use y-axis as the emission direction, we may neglect μ and just keep ϕ. Finally we assume that 2PBM is independent of energy. Then we simplify (67) to get:

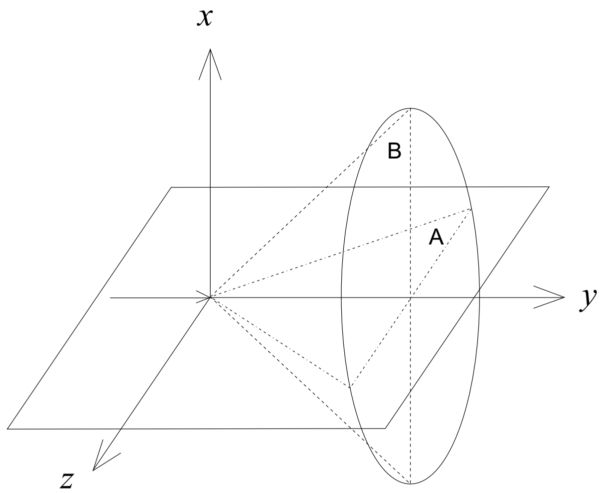

FIGURE 9. Pencil beam

$$cos(\phi)\frac{\partial f(y,z,\phi)}{\partial y} + sin(\phi)\frac{\partial f(y,z,\phi)}{\partial z} = T(E)\frac{\partial^2}{\partial \phi^2} f(y,z,\phi). \tag{70}$$

The equation (70) has been derived and analyzed in [19], [20], [21], [22], [25], [27] and [26] using both spectral and finite element methods. Many different finite element approaches for this model have been discussed in these papers. Comparing BBM and 2PBM, we find that both of them reduce the Fokker-Planck equation from six variables into three variables, but BBM describe a 3D problem which is energy dependent and 2PBM is a projection of 3D problem which is energy independent. In 2PBM we just include the elastic scattering and assume the number of particles will not change, so this model is not sufficient to describe the deep penetration of electrons into medium. But the solution of 2PBM is a part of the solution of the 3D pencil beam model. So we could combine it with BBM to give the solution of the 3D pencil beam model. This process can be viewed as a kind of separation of variables.

2.3. **Bipartition Model.** In this section we will give a brief introduction of the bipartition model based on 1-50 MeV electron transport equation. We compare the bipartition model with the Fokker-Planck equation derived in the last two sections. Bipartition model was presented in 1967 by Luo in [3]. The main idea of this model is to separate the beam into a diffusion group and a straightforward group and deal with them separately. [4, 7] are the two most important papers about bipartition model for electron transport. In [4] Luo used bipartition model for 20 keV-1 MeV electron transport which takes into account both elastic and inelastic scatterings. In [7] Luo extended bipartition model into the energy range 1-50 MeV, considered the influence of the energy-loss straggling, secondary-electron production, and bremsstrahlung. The applications of bipartition model for inhomogeneous problems and ion transport are discussed in [5, 6]. The history and development of the transport theory of charged particles and bipartition model are summarized in [8, 9]. Bipartiton model could also be combined with Fermi-Eyges theory to produce the hybrid electron pencil beam model for 3D problems.

We assume an infinity wide electron beam incident upon the surface of a homogeneous semi-infinite solid, slab $x > 0$ directed in positive x-direction. For forward-peaked electron, one may consider that the material on the left side of the entrance surface to be the same type as the right side, or the left side of the surface is just vacuum. The x axis is along the normal direction of the surface of the solid with the origin on the surface. This is the broad beam model we defined in Section 2.2. The Lewis transport equation, see [4], within the Fokker-Planck frame is given by,

$$\begin{aligned}-\frac{\partial}{\partial E}(\rho_c f) + \mu\frac{\partial f}{\partial x} - \frac{1}{2}\frac{\partial^2}{\partial E^2}(\Omega_c f) + \varphi_r f = &\int_E^{E_0} f(x,\mu,E')\frac{N_A D}{A}\sigma_r(E', E'-E)dE' \\ &+ C_f(x,\mu,E) + \frac{\delta(x)\delta(1-\mu)\delta(E-E_0)}{2\pi},\end{aligned} \tag{71}$$

$$C_f(x,\mu,E) = \int_{4\pi}[f(x,\mu',E) - f(x,\mu,E)]\frac{N_A D}{A}\sigma_{MF}(E, \mathbf{u}\cdot\mathbf{u}')d\mathbf{u}', \tag{72}$$

$$\varphi_r(E) = \frac{N_A D}{A}\int_\epsilon^E \sigma_r(E,T)dT. \tag{73}$$

Comparing (71) with (69), we find out that Luo just did asymptotic approximation for energy. Having emitted a bremsstrahlung photon, the energy spread of the electron is much larger than that for elastic collisions. In this way, Luo assumed that, having emitted a bremsstrahlung photon, both the forward-directed electrons and the diffusion electrons belong to the diffusion electron component. Furthermore, Luo neglected the event of emitting of a photon with energy lower than $\epsilon = 0.02E_0$. Besides, due to the small deflection of recoil electrons he also neglected the direction change after an electron emitted photon. Following the main idea of bipartition model we could split (71) as $f(x,\mu,E) = f_s(x,\mu,t) + f_d(x,\mu,E)$.

$$\begin{aligned}-\frac{\partial}{\partial E}(\rho_c f_s) + \mu\frac{\partial f_s}{\partial x} - \frac{1}{2}\frac{\partial^2}{\partial E^2}(\Omega_c f_s) + \varphi_r f_s = &\int_{4\pi}[f_s(x,\mu',E) - f_s(x,\mu,E)]\frac{N_A D}{A}\sigma_{MF}(E,\mathbf{u}\cdot\mathbf{u}')d\mathbf{u}' \\ &- S_d + \frac{\delta(x)\delta(1-\mu)\delta(E-E_0)}{2\pi},\end{aligned} \tag{74}$$

$$\begin{aligned}-\frac{\partial}{\partial E}(\rho_t f_d) + \mu\frac{\partial f_d}{\partial x} - \frac{1}{2}\frac{\partial^2}{\partial E^2}(\Omega_t f_d) = &\int_{4\pi}[f_d(x,\mu',E) - f_d(x,\mu,E)]\frac{N_A D}{A}\sigma_{MF}(E,\mathbf{u}\cdot\mathbf{u}')d\mathbf{u}' \\ &+ \int_{E+\epsilon}^{E_0} f_s(x,\mu,E')\frac{N_A D}{A}\sigma_r(E',E'-E)dE' + S_d.\end{aligned} \tag{75}$$

Expanding the distribution functions f_s, f_d and S_d into Legendre polynomials, we have

$$
\begin{aligned}
f_s(x,\mu,E) &= \sum_{l=0}^{\infty} \frac{2l+1}{4\pi} p_l(\mu) A_l(x,E),\\
f_d(x,\mu,E) &= \sum_{l=0}^{\infty} \frac{2l+1}{4\pi} p_l(\mu) N_l(x,E),\\
S_d(x,\mu,E) &= \sum_{l=0}^{m} \frac{2l+1}{4\pi} p_l(\mu) S_l(x,E).
\end{aligned}
\tag{76}
$$

Using the partition condition, we have

$$
C_{f_s}(x,\mu_i,E) = S_d(x,\mu_i,E), \qquad i = 0,1,\cdots,m, \tag{77}
$$

$$
S_l(x,E) = -\varphi_l(E) A_l(x,E) - \sum_{l'=m+1}^{\infty} D_{ll'} \varphi_{l'} A_{l'}(x,E). \tag{78}
$$

From (74) to (78) we obtain

$$
\begin{aligned}
&-\frac{\partial}{\partial E}[L(E,\triangle)A_l(x,E)] + \mu_a \frac{\partial A_l}{\partial x} - \frac{1}{2}\frac{\partial^2}{\partial E^2}[\Omega_c A_l(x,E)] + \varphi_r A_l(x,E)\\
&\qquad\qquad = \sum_{l'=m+1}^{\infty} D_{ll'} \varphi_{l'} A_{l'}(x,E) + \delta(x)\delta(E-E_0), \qquad l \le m,\\
&-\frac{\partial}{\partial E}[L(E,\triangle)A_l(x,E)] + \mu_a \frac{\partial A_l}{\partial x} - \frac{1}{2}\frac{\partial^2}{\partial E^2}[\Omega_c A_l(x,E)] + \varphi_r A_l(x,E)\\
&\qquad\qquad = -\varphi_l A_l(x,E) + \delta(x)\delta(E-E_0), \qquad l > m,
\end{aligned}
\tag{79}
$$

$$
\begin{aligned}
&-\frac{\partial \rho_t N_l}{\partial E} + \left[\frac{l+1}{2l+1}\frac{\partial N_{l+1}}{\partial x} + \frac{l}{2l+1}\frac{\partial N_{l-1}}{\partial x}\right]\\
&\qquad = \frac{1}{2}\frac{\partial^2 \Omega_t N_l}{\partial E^2} - \varphi_l N_l + \frac{N_A}{A} D \int_{E+\epsilon}^{E_0} A_l(x,E')\sigma_r(E',E'-E)dE' + S_l, \qquad l = 0,1,\cdots,n.
\end{aligned}
\tag{80}
$$

Compared with Section 2.2 and 2.3, we solve (69) using finite element method and Luo solved (79) and (80) by Fourier transform and Lax-Wendroff scheme. The difference between Fokker-Planck equation and bipartition model is that Luo didn't use asymptotic approximation for angle in (1), he separated large angle scattering from small angle scattering and introduced bipartition condition. The reason is that for low energy electron transport large angle scattering from elastic scattering is important and for this case the Fokker-Planck operator is not an accurate asymptotic approximation of the integral operator. In Section 2.1 we have explained this for the screened Rutherford cross section. But for high energy electron transport and ion transport the situation is somewhat better. In Section 2.1 we check the accuracy of the asymptotic approximation for 1-50 MeV electron transport and we will also check it for ion transport and electron transport in more energy ranges in the future work. In [4] Luo calculated the energy deposition of 1 MeV electrons in carbon, aluminium, copper, tin and lead compared with the Spencer's moment method, and the energy deposition of 0.032, 0.1 MeV electrons compared with Grün's and Huffman's experiments. In [7] Luo calculated the energy deposition of 30 m_0c^2 electrons in water compared with the Spencer's moment method and 10, 20, 40 MeV electrons in water compared with the experimental data. He also calculated the angle distribution at depth x=0.07, 0.017, 0.37, and 0.77 for 10 MeV electrons in water compared with Monte Carlo simulations.

3. Streamline diffusion method

3.1. **Streamline diffusion method.** Both Fermi and Fokker-Planck equations are convection dominated convection-diffusion equations. To obtain approximate solutions for these types of equations, we may use a certain type of the Galerkin method: the streamline diffusion finite element method. Because of a lack of stability of the standard Galerkin finite element method (SGM) , the Galerkin approximation contain oscillations not present in the true solution in convection dominated problems. This has disastrous influence on the performance of an adaptive method leading to refinements in large regions where no refinement is needed. So we need to improve the stability properties of the Galerkin finite element method without sacrificing accuracy. We consider two ways of enhancing the stability of SGM. (a) introduction of weighted least squares terms; (b) introduction of artificial viscosity based on the residual. We refer to the Galerkin finite element method with these modifications as the streamline diffusion method. Both modifications enhance stability without a strong effect on the accuracy.

We begin by describing the Sd-method for an abstract linear problem of the form

$$Au = f, \tag{81}$$

for which SGM reads: find $U \in V_h$ such that

$$(AU, v) = (f, v), \qquad \forall v \in V_h, \tag{82}$$

where A is a linear operator on a vector space V and V_h is a finite dimensional subspace of V. In our problem, A is a convection-diffusion differential operator.

The lease squares method for (81) is to find $U \in V_h$ that minimizes the residual over V_h in an appropriate norm, that is

$$\|AU - f\|^2 = min_{v \in V_h} \|Av - f\|^2. \tag{83}$$

where $\|\cdot\|$ denotes, e.g. the usual L_2 norm.

This is a convex minimization problem and the solution U is characterized by

$$(AU, Av) = (f, Av), \qquad \forall v \in V_h. \tag{84}$$

We now formulate a Galerkin/least squares finite element method for (82) by taking a weighted combination of (83) and (84): compute $U \in V_h$ such that

$$(AU, v) + (\delta AU, Av) = (f, v) + (\delta f, Av), \qquad \forall v \in V_h, \tag{85}$$

where δ is a parameter to be chosen. We may rewrite the relation (85) as

$$(AU, v + \delta Av) = (f, v + \delta Av), \qquad \forall v \in V_h. \tag{86}$$

Adding the artificial viscosity modification yields the Sd-method in abstract form: find $U \in V_h$ such that

$$(AU, v + \delta Av) + (\epsilon \bigtriangledown U, \bigtriangledown v) = (f, v + \delta Av), \qquad \forall v \in V_h, \tag{87}$$

where ϵ is the artificial viscosity defined in terms of the residual $R(U) = AU - f$.

3.2. **Boundary conditions for the broad beam model.** We define the boundary conditions for the broad beam model as the following:

$$\begin{aligned}
\mu\frac{\partial f(x,\mu,E)}{\partial x} =& T(E)\frac{\partial}{\partial\mu}(1-\mu^2)\frac{\partial}{\partial\mu}f(x,\mu,E) + \frac{\partial}{\partial E}[S(E)f(x,\mu,E)] + \frac{\partial^2}{\partial E^2}[R(E)f(x,\mu,E)] \quad (x,\mu,E)\in\Omega \\
& f(0,\mu,E) = g(\mu,E) \qquad (\mu,E)\in[-1,1]\times[0,E_0] \qquad (BC1) \\
& f(x_0,\mu,E) = 0 \qquad (\mu,E)\in[-1,1]\times[0,E_0] \qquad (BC2) \\
& \frac{\partial}{\partial\mu}f(x,1,E) = 0 \qquad (x,E)\in(0,x_0)\times(0,E_0] \qquad (BC3) \\
& f(x,-1,E) = 0 \qquad (x,E)\in(0,x_0)\times(0,E_0] \qquad (BC4) \\
& \frac{\partial}{\partial E}f(x,\mu,E_0) = 0 \qquad (x,\mu)\in(0,x_0)\times(-1,1] \qquad (BC5) \\
& f(x,\mu,0) = 0 \qquad (x,\mu)\in(0,x_0)\times[-1,1] \qquad (BC6).
\end{aligned} \tag{88}$$

3.3. **Results.** We use Sd-method to solve (88) and integrate $f(x, \mu, E)$ about μ and E to get the energy and angular distributions for different depths. We compare 10, 20, 30 MeV electron transport in water with the bipartition model and MC. We neglect the secondary particle transport. In Fig. 11, 14 and 17 we could find that our results are very close to MC, only the positions of the maximum values are different. The reason is that the stopping power we have used is somewhat different from that of MC. We use the same stopping power with the bipartition model, so we could find that the positions of the maximum values are very close as in Fig. 10, 13 and 16. And the bipartition model use CSDA and neglect the particles which have larger changes for energy and angle. So the energy distributions are very narrow and the maximum values decrease more quickly. Similar phenomena appears for the angular distributions in Fig. 12, 15, and 18.

4. Conclusion

In this thesis, we use the streamline diffusion method to calculate the energy and angular distributions for the electron transport equation and compared the results with those obtained by bipartition model and Monte Carlo simulation. In our knowledge, this approach is not considered elsewhere. This is our first contribution in this field. Our ambition is to solve 3D pencil beam model, and show the advantages of FEM in particular in the cases of inhomogeneous data and media as well as irregular geometry. We shall also extend our work to ion transport and include secondary particle transport. More mathematical discussions will also follow concerning the error analysis for FEM applied to these models.

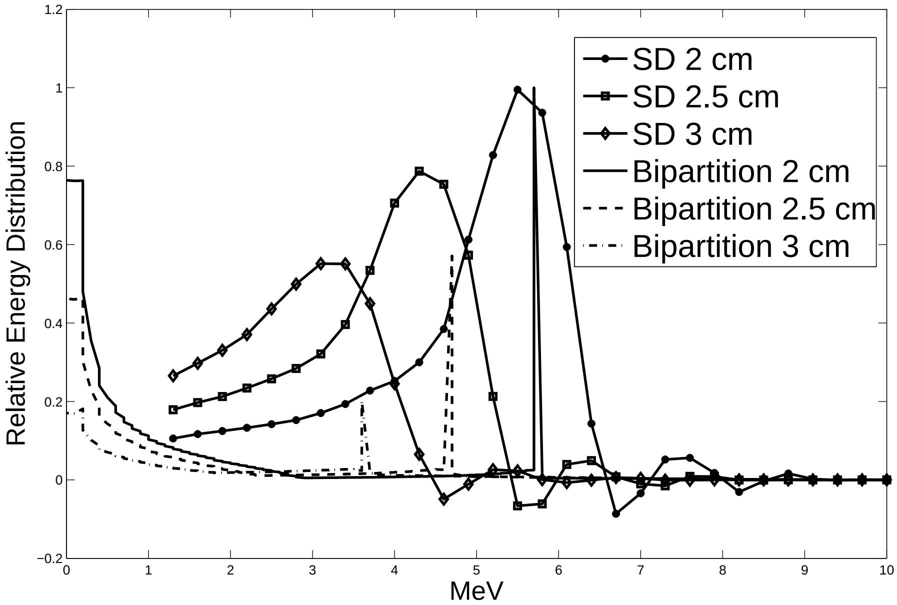

FIGURE 10. 10MeV Relative Energy Distribution

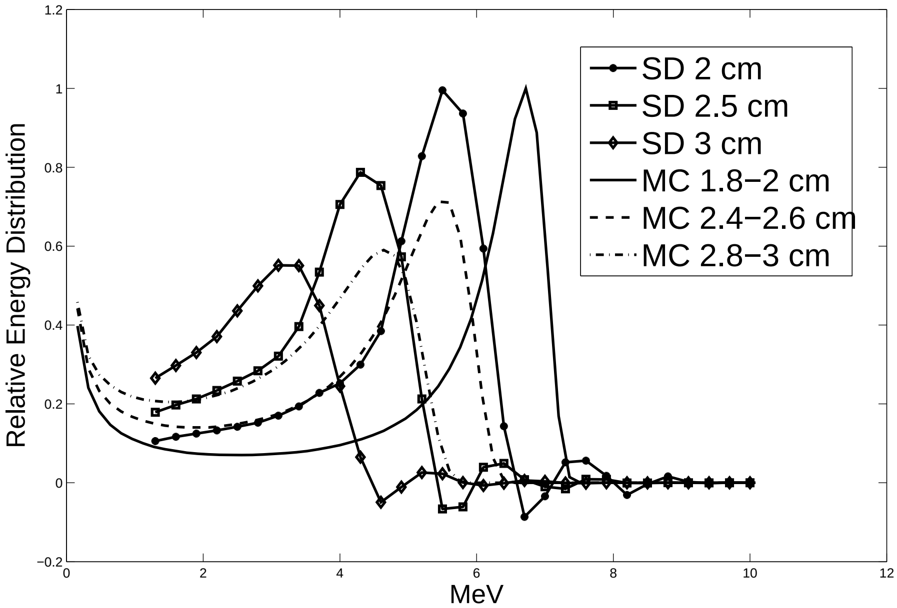

FIGURE 11. 10MeV Relative Energy Distribution

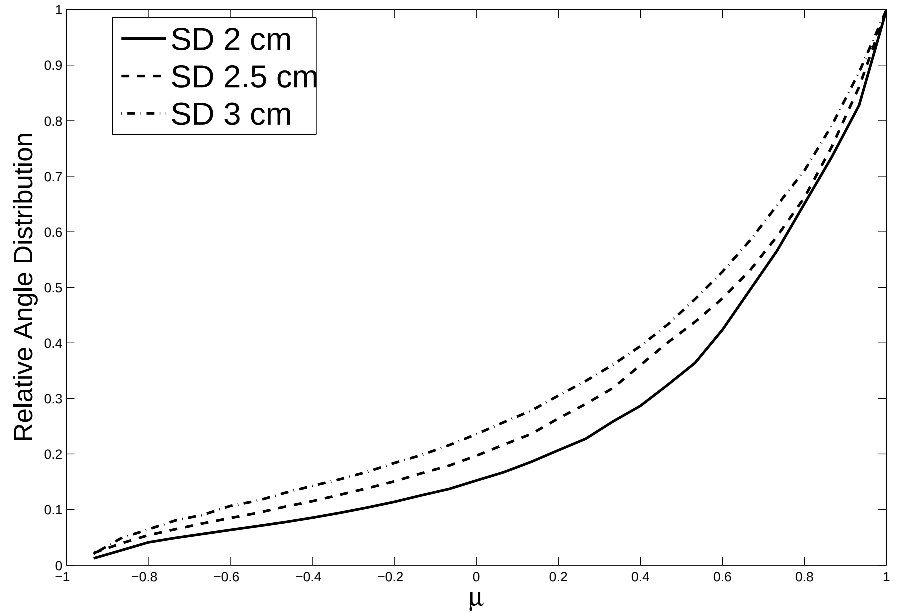

FIGURE 12. 10MeV Relative Angle Distribution

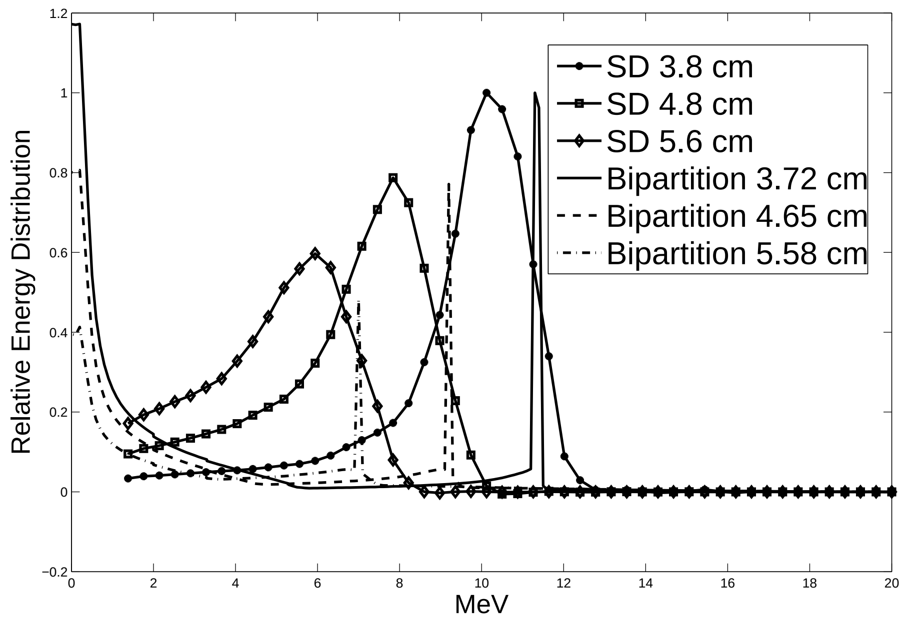

FIGURE 13. 20MeV Relative Energy Distribution

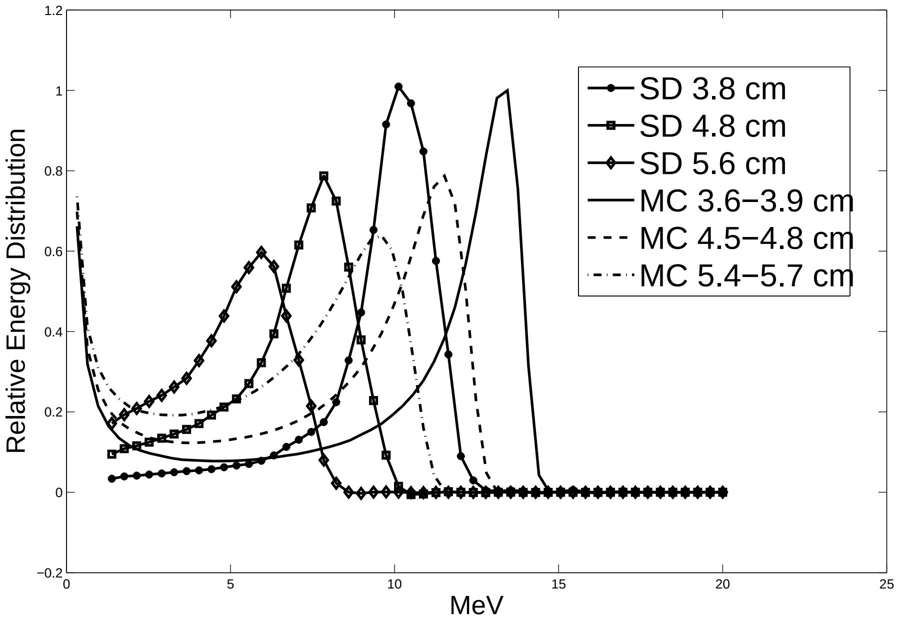

Figure 14. 20MeV Relative Energy Distribution

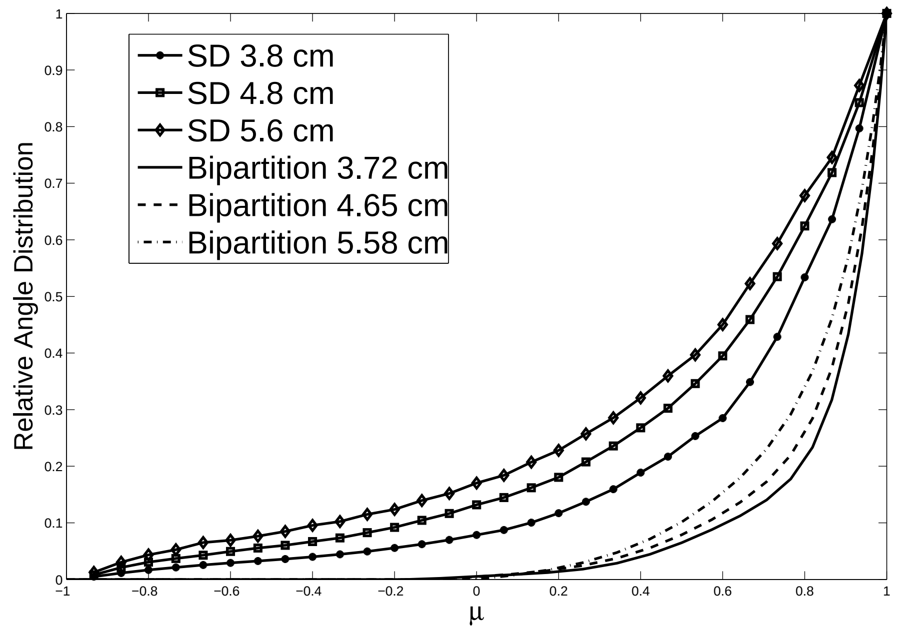

Figure 15. 20MeV Relative Angle Distribution

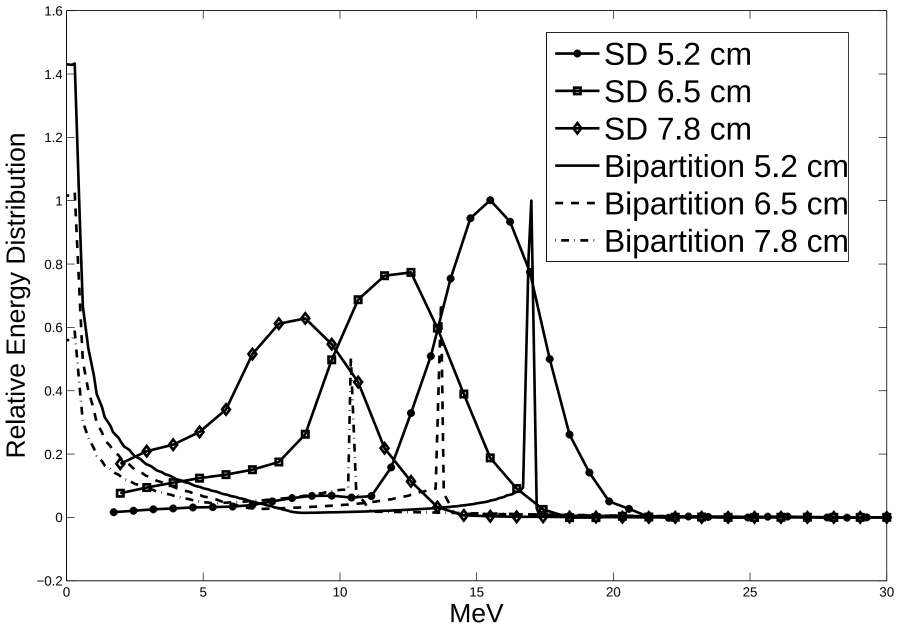

FIGURE 16. 30MeV Relative Energy Distribution

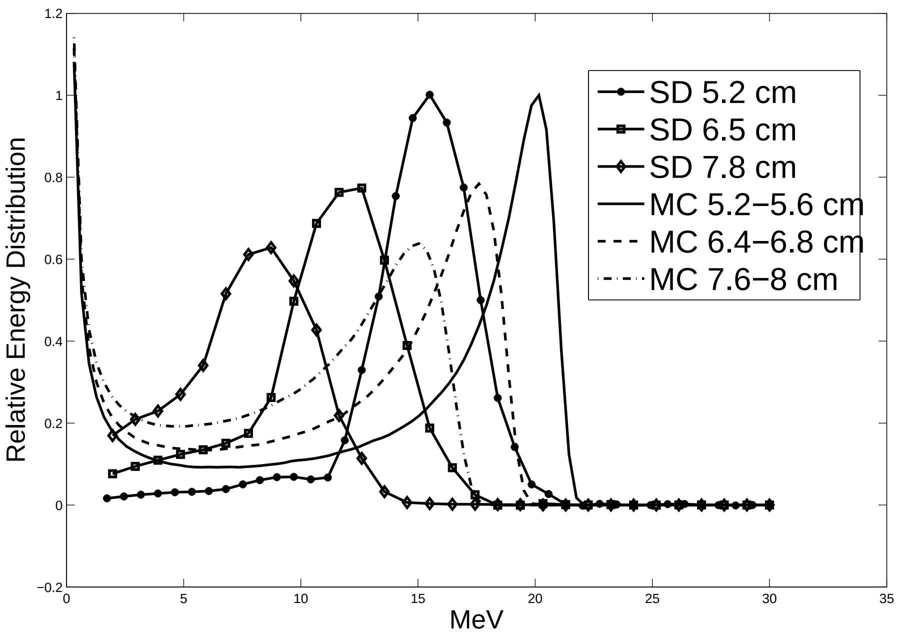

FIGURE 17. 30MeV Relative Energy Distribution

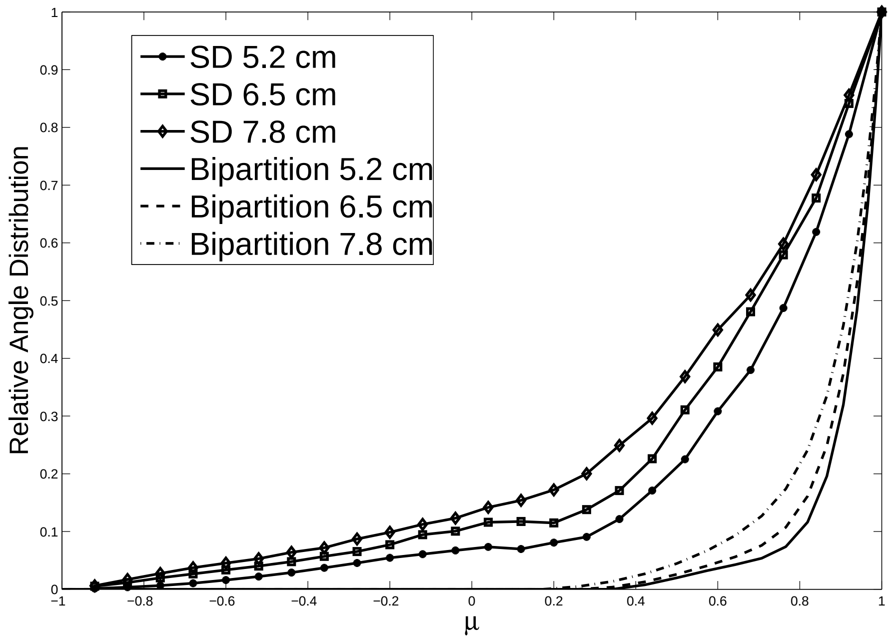

FIGURE 18. 30MeV Relative Angle Distribution

5. ACKNOWLEDGMENT

I am very grateful to Associate Professor Mohammad Asadzadeh for introducing me to the subject of this thesis, and for his encouragement to this work. Thanks are also due to Professor Anders Brahme and Johanna Kempe in Karolinska Institute, and Professor Zhengming Luo and Associate Professor Chengjun Gou in Sichuan University for instructive discussions and supplying the Monte Carlo and bipartiton model data. This work is supported by Gothenburg Mathematical Modelling Center (GMMC).

REFERENCES

[1] Jiping Xin, Chengjun Gou. *Comparsion of Streamline Diffusion Method and Bipartition Model for Electron Transport*, In peraperation.

[2] Jiping Xin, Johanna Kempe. *Comparsion of Streamline Diffusion Method and Fourier Transform for Ion Transport*, In peraperation.

[3] Z.-M. Luo, *A theory of electron multiple scattering and electron energy losses*, In collected papers in Atomic Energy and Technology (Atomic Energy Press, Beijing, 1976).

[4] ______, *Improved bipartition model of electron transport (I). A general formulation*, Physical Review B (1985) 32 812.

[5] ______, *Improved bipartition model of electron transport (II). Application to inhomogeneous media*, Physical Review B (1985) 32 824.

[6] Z.-M. Luo and S.M. Wang, *Bipartiton model of ion transport: An outline of new range theory for light ions*, Physical Review B (1987) 36 1885.

[7] Z.-M. Luo and A. Brahme, *High-energy electron transport*, Physical Review B (1992) 46 15739.
[8] Z.-M. Luo and A. Brahme, *An overview of the transport theory of charged particles*, Radiat. Phys. Chem. (1993) 41 673.
[9] Z.-M. Luo, *An overview of the bipartition model for charged particle transport*, Radiat. Phys. Chem. (1997) 53 305.
[10] Z.-M. Luo, D. Jette, and S. Walker, *Electron dose calculation using multiple-scattering theory: A hybrid electron pencil-beam model*, Med. Phys. (1998) 25 1954.
[11] C.-J. Gou, *Studies on the application of electron hybrid pencil-beam model to 3D dose calculation*, PhD thesis.
[12] Z.-M. Luo, *Algorithm Investigation in Phoenix Treatment Planning system* , Seminar in Chalmers.
[13] Z.-M. Luo and C.-J. Gou, *Photon transport*, Private communication.
[14] W.A. McKinley and H. Feshbach, *The Coulomb Scattering of Relativistic Electrons by Nuclei* , Phys. Rev. 74(1759), 1948.
[15] G. Moliere and Z. Naturforsch, A 2, 133(1947), 3, 78(1948).
[16] H. A. Bethe and J. Ashkin, in Passage of Radiation Through Matter, Experimental Nuclear Physics Vol. 1, edited by E. Segre(Wiley, New York, 1960).
[17] W. Heitler, The Quantum Theory of Radiation, 2nd ed. (Oxford University Press, London, 1936).
[18] S. M. Seltzer and M. J. Berger, Int. J. Appl. Radiat. Isot. 33, 1219 (1982).
[19] Asadzadeh, M., *Streamline diffusion methods for the Fermi and Fokker-Planck Equations*, Transport Theory and Statistical Physics, (1997) 319-340.
[20] ———, *On convergence of FEM for the Fokker-Planck equation*, Proceedings of 20th International Symposium on Rarefied Gas Dynamics, ed by C. Shen, Peking University Press, Beijing, (1997), 309-314.
[21] ———, *Characteristic Methods for Fokker-Planck and Fermi Pencil Beam Equations*, Proceedings of 21th International Symposium on Rarefied Gas Dynamics, ed. by R. Brun et al , Vol II, 205-212, Marseille 1998.
[22] ———,*A posteriori error estimates for the Fokker-Planck and Fermi pencil beam equations*, Mathematical Models and Methods in Applied Science, 10(2000), pp. 737–769.
[23] ———, *The Fokker-Planck Operator as an Asymptotic Limit in Anisotropic Media*, Math. Comput. Modelling, 35 (2002) pp 1119-1133.
[24] Asadzadeh, M. and Sopasakis, A., *On Fully Discrete Schemes for the Fermi Pencil-Beam Equations*, Computer Methods in Applied Mechanics and Engineering 191, (2002), 4641-4659.
[25] Asadzadeh, M., *On the stability of characteristic schemes for the Fermi equation* , Appl. Comput. Math., 1 (2002). 158–174.
[26] Asadzadeh, M. and E. W. Larsen, *Linear particle transport in flatland*, Preprint 2006:34. Department of Mathematics, Chalmers University of Technology, Göteborg University.
[27] ———, *Linear transport equations in flatland with small angular diffusion and their finite element approximations*, Math and Computer Mod., 47(2008), 495-514.
[28] S. Chandrasekhar, *Stochastic problems in physics and astronomy*, Rev. Modern Phys. 15(1943), pp 1-89.
[29] J.Morel, *Fokker-Planck calculations using standard discrete ordinate transport codes*, Nuclear Sci. Engrg. 79(1981), pp 340-356.
[30] Pomraning, G. C., *Flux-limited diffusion and Fokker-Planck equations*, Nuclear Sci. Engrg. 85(1983), pp 116-126.
[31] K. Przybylski and J.Ligou, *Numerical analysis of the Boltzmann equation including Fokker-Planck terms*, Nuclear Sci. Engrg. 81(1982), pp 92-109.
[32] M. Rosenbluth, W.M. MacDonald and D.L. Judd, *Fokker-Planck equation for an inverse-square force*, Phys. Rev. 107(1957), pp 1-6.
[33] Pomraning, G. C., *The Fokker-Planck Operator as an Asymptotic Limit*, Math. Models Methods Appl. Sci. 2(1992), pp 21-36.

[34] ______, *An asymptotic model for the spreading of a collimated beam*, Nuclear Sci. Engrg. 347(1992), pp 112.

[35] Börgers, C. and Larsen, E. W., *Asymptotic derivation of the Fermi pencil beam approximation*, Nuclear Science and Engineering (1996) vol.123 16 pp. 343–357.

[36] ______, *The transversely integrated scalar flux of a narrowly focused particle beam*, SIAM J. Appl. Math., 55,1 (1995).

[37] ______, *The fermi pencil beam approximation*, Proc. Int. Conf. Mathematics and Computations, Reactor Physics, and Environmental Analyses, Portland, Orego, April 30-May 4, 1995, Vol. 2, p.847(1995).

[38] ______, *On the accuracy of the Fokker-Planck and Fermi pencil beam equations for charged particle transport*, Med. Phys. .

[39] Leonard Eyges, *Multiple scattering with energy loss*, Phys. Rev., 74, 1534-1535(1948).

[40] B. Rossi and K. Greisen, *Cosmic-ray theory*, Rev. Mod. Phys., 240, 265-268(1941).